

AutoHFormer: Efficient Hierarchical Autoregressive Transformer for Time Series Prediction

Qianru Zhang^{✉*}, Honggang Wen^{✉*}, Ming Li^{✉†}, Dong Huang^{✉‡}, Siu-Ming Yiu^{✉*§}

Christian S. Jensen^{✉††}, IEEE Fellow, Pietro Liò^{✉¶§}

^{*}School of Computing and Data Science, The University of Hong Kong (HKU)

[†]Zhejiang Key Laboratory of Intelligent Education Technology and Application, Zhejiang Normal University (ZJNU)

[‡]Department of Computer Science, National University of Singapore (NUS)

^{††}Department of Computer Science, Aalborg University (AU)

[¶]Department of Computer Science and Technology, Cambridge University (Cambridge)

Abstract—Time series forecasting requires architectures that simultaneously achieve three competing objectives: (1) strict temporal causality for reliable predictions, (2) sub-quadratic complexity for practical scalability, and (3) multi-scale pattern recognition for accurate long-horizon forecasting. We introduce AutoHFormer, a hierarchical autoregressive transformer that addresses these challenges through three key innovations: 1) Hierarchical Temporal Modeling: Our architecture decomposes predictions into segment-level blocks processed in parallel, followed by intra-segment sequential refinement. This dual-scale approach maintains temporal coherence while enabling efficient computation. 2) Dynamic Windowed Attention: The attention mechanism employs learnable causal windows with exponential decay, reducing complexity while preserving precise temporal relationships. This design avoids both the anti-causal violations of standard transformers and the sequential bottlenecks of RNN hybrids. 3) Adaptive Temporal Encoding: a novel position encoding system is adopted to capture time patterns at multiple scales. It combines fixed oscillating patterns for short-term variations with learnable decay rates for long-term trends. Comprehensive experiments demonstrate that AutoHFormer 10.76× faster training and 6.06× memory reduction compared to PatchTST on PEMS08, while maintaining consistent accuracy across 96-720 step horizons in most of cases. These breakthroughs establish new benchmarks for efficient and precise time series modeling. Implementations of our method and all baselines in hierarchical autoregressive mechanism are available at <https://github.com/lizzyhku/Autotime>.

I. INTRODUCTION

Time series forecasting [1, 2, 3, 4, 5] stands as a fundamental pillar of modern predictive analytics, enabling data-driven decision making across numerous mission-critical domains. As demonstrated in recent literature [6], this task has become increasingly vital in our data-rich era. In financial markets [7, 8], accurate forecasting drives risk management strategies. Energy sector applications require precise demand predictions to optimize renewable integration. Transportation systems [9, 10] rely on temporal pattern analysis for traffic flow optimization. The importance of time series analysis also extends to public safety through crime prediction [6]. These diverse applications share a common need: the ability

to extract meaningful patterns from temporal data to inform proactive decision-making.

The evolution of time series forecasting has been significantly advanced by Transformer architectures [11], yet persistent limitations hinder their practical deployment. As shown in Figure 1, conventional Transformers suffer from **anti-causal attention flows**, violating the fundamental $p(x_t|x_{<t})$ principle through bidirectional information propagation, which is particularly detrimental in autoregressive settings. Simultaneously, RNN-Transformer hybrids impose **sequential computation bottlenecks** ($\mathcal{O}(L)$ time steps) (L is the sequence length) that eliminate parallel processing advantages. Three fundamental shortcomings emerge from this architectural landscape: (1) **Quadratic Complexity**: Standard self-attention’s $\mathcal{O}(L^2)$ memory and computation requirements render long-sequence processing infeasible; (2) **Error Propagation**: Autoregressive approaches accumulate prediction errors exponentially across time steps; (3) **Temporal Representation Rigidity**: Fixed attention patterns fail to adapt to varying time scales and event frequencies.

While recent innovations like Informer [12] and Pyraformer [13] address individual aspects, they fail to address three competing demands simultaneously: *computational efficiency* (sub-quadratic complexity), *temporal coherence* (strict causality), and *multi-scale pattern capture* (from minute-level transients to daily periodicity). To resolve this trilemma, we propose **AutoHFormer**, a novel architecture that addresses three critical limitations of existing approaches via three innovations: (1) **Sub-quadratic Complexity and Temporal Coherence Maintenance**. The Dynamic Windowed Attention Mechanism achieves $\mathcal{O}(LW)$ (W denotes the window size) complexity via learnable causal windows, maintaining temporal coherence through: (i) strict architectural causality ($p(x_t|x_{<t})$), (ii) exponential decay ($\tau(t, t') = e^{-\gamma|t-t'|}$) to weight dependencies by proximity (shown in Figure 1). This design ensures sub-quadratic efficiency ($\lim_{L \rightarrow \infty} LW/L^2 = 0$) while preserving parallelizability. The constant memory footprint ($\mathcal{O}(W)$ per token) enables efficient deployment without sacrificing temporal relationships. (2) **Error-Resistant Hierarchical Refinement**. Autoregressive

^{||}Equal Contribution.

[§]Corresponding author.

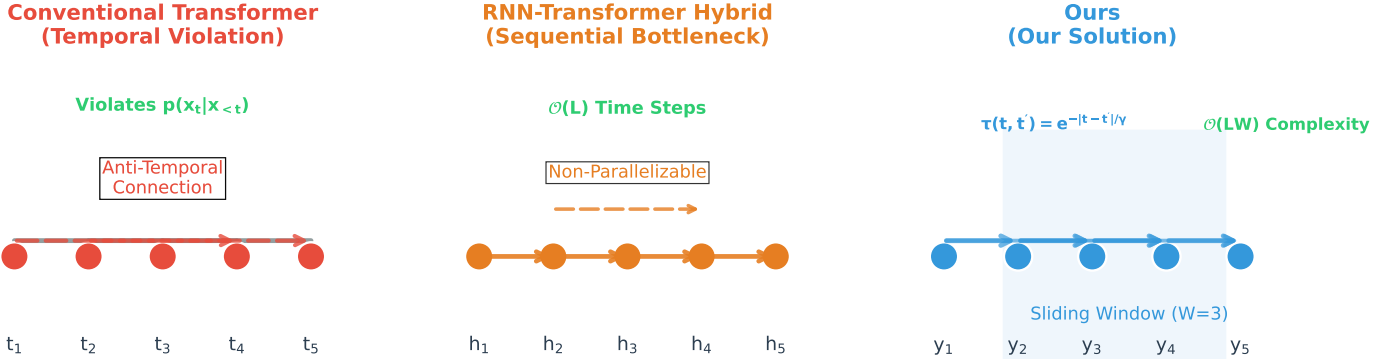


Fig. 1. Architectural comparison of time series modeling approaches: (a) **Conventional Transformer** suffers from anti-causal attention flows (red dashed arrows) that violate the fundamental autoregressive principle $p(x_t | x_{<t})$. (b) **RNN-Transformer Hybrid** enforces causality through sequential processing (orange solid arrows) but introduces an $\mathcal{O}(L)$ computational bottleneck that prevents parallel training. (c) **Ours** (our solution) combines: ① Strictly causal attention within a sliding window W (blue shaded region), ② Exponentially decaying attention weights $\tau(t, t') = e^{-|t-t'|/\gamma}$ (visualized by arrow opacity gradient), and ③ $\mathcal{O}(LW)$ complexity through windowed parallel processing. The thickness of blue arrows represents attention magnitude, demonstrating our model’s ability to simultaneously maintain temporal causality while enabling efficient parallel computation.

approaches suffer from compounding prediction errors. Motivated by this, we propose dual-phase architecture with (i) segment-level autoregression and (ii) intra-segment stepwise correction via normalized residuals. Meanwhile, for inter-segment level autoregression, layer-normalized residual updating and moving average smoothing are proposed to enable stable prediction within segment. It not only reduces error propagation specifically in long-term forecasts, but also provides stable long-term prediction. (3) **Adaptive Temporal Position Encoding**. Fixed positional representations fail to capture varying temporal scales. Hybrid system combining sinusoidal patterns with learned decay coefficients. It captures both local dynamics through high-frequency sinusoidal components and global trends via learned decay rates. The synergistic integration of these components establishes **AutoHFormer** as a new paradigm in temporal modeling, achieving better prediction performance in comparable complexity.

We summarize our contributions as follows:

- **An Efficient and Unified Hierarchical Autoregressive Transformer for Time Series Prediction.** We propose a hierarchical autoregressive framework via block (segment) processing and step refinement for efficient long-horizon prediction.
- **Efficient Dynamic Attention with Temporal Coherence Maintenance.** A memory-efficient attention mechanism featuring is implemented with Learnable causal windows and Exponential decay.
- **Adaptive Temporal Encoding for Multi-scale Patterns and Short Transients.** We adopts relative positive temporal encoding with learned decay coefficients, which captures varying temporal scales including short transients and multi-scale patterns.
- **Comprehensive Empirical Validation.** Through extensive experiments on benchmark datasets, **AutoHFormer** demonstrates superior performance compared to 8 state-of-the-art baselines, including transformer

variants (iTransformer, Informer, Autoformer) and modern architectures (PatchTST, TimeMixer), particularly excelling in long-sequence scenarios (720+ prediction steps). Implementations of our method and all baselines in hierarchical autoregressive mechanism are available at <https://github.com/lizzyhku/Autotime>.

II. METHOD

A. Overview of **AutoHFormer**

The **AutoHFormer** framework introduces a novel hierarchical autoregressive transformer that fundamentally advances time series forecasting through three key innovations. **First**, our hierarchical architecture combines segment-wise processing with stepwise refinement to eliminate error propagation in long-horizon predictions. **Second**, the optimized windowed attention mechanism employs learnable causal windows $\mathcal{W}_t = [t - w, t]$ (W : window size) to achieve $\mathcal{O}(LW)$ complexity while preserving temporal coherence ($p(x_t | x_{<t})$). The resulting system maintains sub-quadratic scaling ($LW \ll L^2$ for $L \gg W$) with full parallelizability, while the fixed per-token memory requirement ($\mathcal{O}(W)$) ensures hardware efficiency. **Third**, adaptive temporal position encodings capture multi-scale patterns and short transients through hybrid sinusoidal-decay embeddings. Theoretically grounded in Section II-H and empirically validated in Section III, **AutoHFormer** demonstrates: (1) $10.76\times$ faster training than conventional transformer-based PatchTST on PEMS08, (2) consistent accuracy across 96-720 step horizons in most of cases, and (3) $6.06\times$ memory reduction than PatchTST on PEMS08 establishing new standards for efficient and accurate temporal modeling.

B. Preliminary

1) *Autoregressive (AR) Mechanism.*: The $AR(p)$ model expresses the current value X_t as a linear combination of its p previous values plus a stochastic error term:

$$X_t = c + \phi_1 X_{t-1} + \phi_2 X_{t-2} + \dots + \phi_p X_{t-p} + \epsilon_t \quad (1)$$

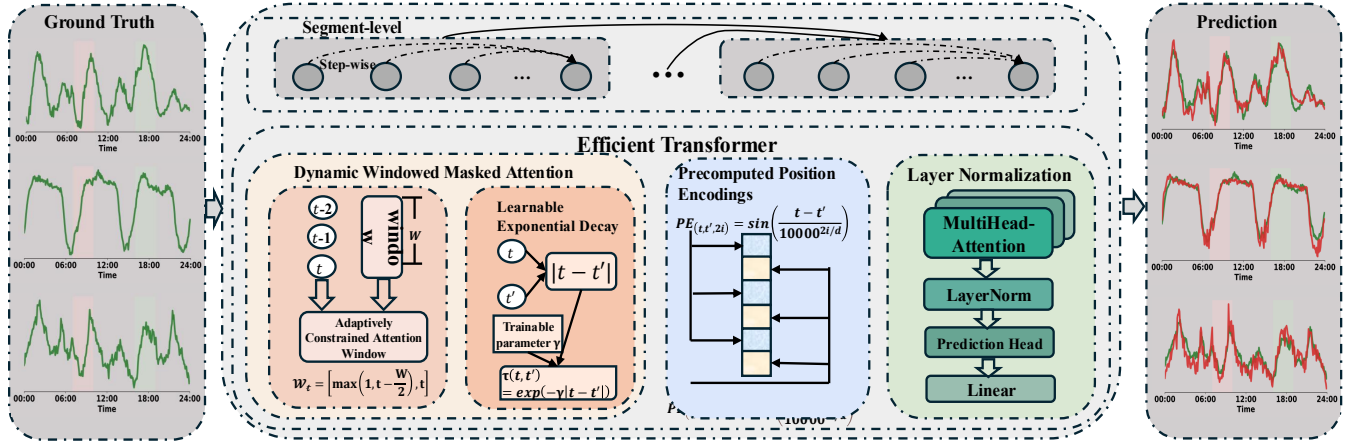


Fig. 2. The Overview of **AutoHFormer**. The left part is the input time series data. The right part is the prediction. For the middle part, (a) the top component is hierarchical autoregressive mechanism including segment-level part and step-wise part. (b) For the bottom part of the middle, there are three key components: (1) a dynamic windowed attention mechanism that computes localized attention patterns with adaptive window sizing, (2) precomputed relative position encodings that capture temporal relationships through sinusoidal embeddings, and (3) a series of several sub-models (efficient transformer) with layer normalization that progressively refine feature representations while maintaining strict causality. The complete system transforms raw input sequences into accurate predictions through this optimized transformer-based pipeline, achieving both computational efficiency and modeling precision.

Here c denotes the constant term (unconditional mean when $\phi_i = 0$). ϕ_i denotes autoregressive coefficients (weights for past values). $\epsilon_t \sim \mathcal{N}(0, \sigma^2)$ denotes the white noise innovation. The model captures how past values influence the present through the weights ϕ_i . Higher absolute values of ϕ_i indicate stronger dependence on the i -th lag.

For a time series with T observations, we can express the autoregressive mechanism in matrix form:

$$\begin{bmatrix} X_{p+1} \\ X_{p+2} \\ \vdots \\ X_T \end{bmatrix} = \Omega \begin{bmatrix} c \\ \phi_1 \\ \phi_2 \\ \vdots \\ \phi_p \end{bmatrix} + \begin{bmatrix} \epsilon_{p+1} \\ \epsilon_{p+2} \\ \vdots \\ \epsilon_T \end{bmatrix} \quad (2)$$

where $\Omega = \begin{bmatrix} 1 & X_p & X_{p-1} & \cdots & X_1 \\ 1 & X_{p+1} & X_p & \cdots & X_2 \\ \vdots & \vdots & \vdots & \ddots & \vdots \\ 1 & X_{T-1} & X_{T-2} & \cdots & X_{T-p} \end{bmatrix}$. Here Equation 2 contains lagged values of X_t and enables efficient computation of parameters via least squares. Meanwhile, $T > 2p$ is required for identifiability. An AR process is stationary if all roots of the characteristic polynomial lie outside the unit circle:

$$1 - \phi_1 z^{-1} - \phi_2 z^{-2} - \cdots - \phi_p z^{-p} \neq 0 \quad \text{for } |z| \leq 1 \quad (3)$$

2) Problem Definition: Given an input sequence $\mathbf{X}_{1:L} \in \mathbb{R}^{L \times V}$ with V variates, we predict K consecutive segments $\{\hat{\mathbf{Y}}_1, \dots, \hat{\mathbf{Y}}_K\}$ where each segment $\hat{\mathbf{Y}}_h \in \mathbb{R}^{H \times V}$ has fixed horizon H . The task is to learn two mapping functions \mathcal{F} and \mathcal{G} following a two-level autoregressive process:

1) Segment-level Autoregression:

$$\hat{\mathbf{Y}}_h = \mathcal{F}(\mathbf{X}_{1:L}, \hat{\mathbf{Y}}_{1:h-1}) \quad \forall h \in \{1, \dots, K\} \quad (4)$$

2) Step-wise Generation within each segment:

$$\hat{y}_{(h-1)H+t} = \mathcal{G}(\mathbf{X}_{1:L}, \hat{\mathbf{Y}}_{1:h-1}, \hat{y}_{(h-1)H+1}, \dots, \hat{y}_{(h-1)H+t-1}) \quad \forall t \in \{1, \dots, H\} \quad (5)$$

The model architecture employs several key design parameters to govern its forecasting behavior. The input window size L controls the amount of historical context used for predictions, while the segment length H determines the granularity of each autoregressive prediction block. Together, these parameters enable flexible control over the total prediction horizon $T_{\text{total}} = K \times H$, where K represents the number of autoregressive segments. Crucially, the model maintains strict temporal causality by enforcing the $t' < t$ ordering constraint at both the segment and intra-segment levels, ensuring that predictions only depend on past observations and never future information. This hierarchical causal structure preserves the fundamental time-series forecasting requirement while enabling efficient block-wise processing.

The hierarchical objective function captures both segment-level and step-wise accuracy:

$$\mathcal{L} = \underbrace{\sum_{h=1}^K \alpha_h}_{\text{Segment weights}} \underbrace{\sum_{t=1}^H \lambda_t \|\hat{y}_{(h-1)H+t} - y_{(h-1)H+t}\|_2^2}_{\text{Step-wise loss}} \quad (6)$$

Here $\alpha_h = \gamma^{h-1}$ implements temporal discounting across segments ($\gamma \in (0, 1]$). λ_t adjusts importance of early vs. late predictions within segments

C. Hierarchical Autoregressive Generative Mechanism

Effective time series forecasting requires balancing three competing demands: (1) preserving exact temporal causality, (2) maintaining computational efficiency for long sequences, and (3) capturing multi-scale temporal patterns. Traditional

approaches struggle with this triad-single-shot methods violate causality through bidirectional attention, while conventional autoregressive models suffer from error accumulation and quadratic complexity. **AutoHFormer** addresses these limitations through a hierarchical decomposition that enforces strict Markov dependencies at two levels:

$$p(\hat{\mathbf{Y}}_h | \mathbf{X}_{1:L}, \hat{\mathbf{Y}}_{1:h-1}) \prod_{t=1}^H p(\hat{y}_{(h-1)H+t} | \mathbf{X}_{1:L}, \hat{\mathbf{Y}}_{1:h-1}, \hat{y}_{(h-1)H+1:t-1}) \quad (7)$$

This dual-scale formulation combines the efficiency of block processing with the precision of step-wise refinement.

The hierarchical autoregressive mechanism generates predictions through a two-level procedure that maintains strict temporal causality. For each segment $h \in \{1, \dots, K\}$ with fixed length H :

1) **Segment Initialization:**

$$\hat{\mathbf{Y}}_h^{init} = \mathcal{F}_\theta(\mathbf{X}_{1:L}, \hat{\mathbf{Y}}_{1:h-1}) \in \mathbb{R}^{H \times d} \quad (8)$$

where the context $\mathbf{C}_h = \text{Concat}(\mathbf{X}_{1:L}, \hat{\mathbf{Y}}_{1:h-1}) \in \mathbb{R}^{(L+(h-1)H) \times d}$ accumulates all historical data and previous segments.

2) **Step-wise Refinement** within segment h :

$$\hat{y}_{(h-1)H+t} = \mathcal{G}_\phi(\mathbf{C}_h, \hat{y}_{(h-1)H+1}, \dots, \hat{y}_{(h-1)H+t-1}) \quad (9)$$

$\forall t \in \{1, \dots, H\}$

implemented through:

$$\begin{aligned} \mathbf{o}_t &= \text{WindowedAttention}(\mathbf{C}_h^t, \mathbf{C}_h^t, \mathbf{C}_h^t; A) \\ \mathbf{f}_t &= \text{FFN}(\text{LayerNorm}(\mathbf{o}_t + \mathbf{C}_h^t[-1])) \\ \hat{y}_{(h-1)H+t} &= W_o \mathbf{f}_t[-1], \quad W_o \in \mathbb{R}^{d \times V} \end{aligned} \quad (10)$$

where $\mathbf{C}_h^t = \text{Concat}(\mathbf{C}_h, \hat{y}_{(h-1)H+1}, \dots, \hat{y}_{(h-1)H+t-1})$.

The complete prediction $\hat{\mathbf{Y}} = \{\hat{\mathbf{Y}}_h\}_{h=1}^K$ preserves the autoregressive property $p(\hat{y}_{(h-1)H+t} | \mathbf{X}_{1:L}, \hat{\mathbf{Y}}_{1:h-1}, \hat{y}_{(h-1)H+1}, \dots, \hat{y}_{(h-1)H+t-1})$.

Our autoregressive design offers several key advantages for time series prediction: (1) Error Mitigation through iterative refinement, where each prediction step incorporates previously generated outputs, reducing compounding errors common in long-horizon forecasting; (2) Computational Efficiency via shared transformer weights across time steps, maintaining linear complexity relative to prediction horizon; (3) Temporal Coherence by strictly enforcing causality through attention masking, preventing information leakage while preserving sequential dependencies; (4) Adaptability to variable context lengths through dynamic window expansion, allowing flexible conditioning on both past observations and intermediate predictions. The combination of layer normalization and residual connections further ensures stable gradient flow during backpropagation through extended sequences. Compared to conventional one-shot prediction approaches, this architecture demonstrates superior performance in maintaining temporal consistency while scaling efficiently to long-range forecasting tasks.

D. Enhanced Transformer

1) **Dynamic Windowed Masked Attention (DWMA):** Time series forecasting demands efficient modeling of hierarchical temporal patterns, where both fine-grained fluctuations and coarse-grained trends jointly determine future states. Existing attention mechanisms [11] fundamentally struggle with this multi-scale requirement due to either quadratic complexity ($\mathcal{O}(L^2)$) or information loss in simplified approximations. Our DWMA breakthrough addresses these limitations via: **i) Adaptively Constrained Attention Windows:** The designation of adaptively constrained attention window is shown as $\mathcal{W}_t = [\max(1, t - \frac{W}{2}), t]$, which establishes dynamic receptive fields that maintain strict causality while enabling $\mathcal{O}(LW)$ computational complexity. The window size W acts as a hyperparameter controlling the trade-off between context range and efficiency. **ii) Learnable Exponential Decay:** It introduces position-sensitive weighting via $\tau(t, t') = \exp(-\gamma|t - t'|)$, where the trainable parameter γ automatically adapts to dataset characteristics. This creates continuous attention spectra that emphasize recent patterns while preserving access to critical long-range dependencies.

DWMA's hybrid design achieves superior efficiency-accuracy trade-offs compared to vanilla attention [11]. The decay mechanism automatically adjusts to diverse temporal patterns, which enables our model to have better performance in time series datasets.

2) **Precomputed Position Encodings:** In time series prediction tasks, capturing the relative positions of time steps is critical for modeling temporal dependencies effectively. Relative positions incorporate temporal order information with adaptive attention decay within localized contexts \mathcal{W}_t . It operates on-the-fly for each window $\mathcal{W}_t = \{t' | \max(1, t - W/2) \leq t' \leq t\}$, and the encoding matrix is denoted as $\mathbf{R}_t \in \mathbb{R}^{|\mathcal{W}_t| \times d}$. Traditional position encoding methods, such as absolute positional encodings, fail to explicitly model the relative distances between time steps, which are essential for tasks like prediction and anomaly detection. To address this, we propose Precomputed Position Encodings (PPE), which explicitly encode the relative positions of all pairs of time steps (t, t') using sinusoidal functions. The encoding for dimension i is defined as:

$$\begin{aligned} PE_{(t, t', 2i)} &= \sin\left(\frac{t - t'}{10000^{2i/d}}\right) \\ PE_{(t, t', 2i+1)} &= \cos\left(\frac{t - t'}{10000^{2i/d}}\right) \end{aligned} \quad (11)$$

where d is the embedding dimension, and $i = 0, \dots, d/2 - 1$. These encodings are continuous and periodic, enabling the model to generalize to sequences of varying lengths and capture long-range dependencies. By precomputing these encodings for all pairs (t, t') and storing them in a lookup table $\mathbf{PE} \in \mathbb{R}^{L \times L \times d}$, where:

$$\mathbf{PE}_{t, t'} = [PE(t, t', 0), PE(t, t', 1), \dots, PE(t, t', d-1)]^\top, \quad (12)$$

We avoid redundant computations during training and inference, significantly improving efficiency. The key advantage

of PPE lies in its ability to enhance the model’s temporal awareness without increasing computational complexity. During the attention computation, the relative position encodings $\mathbf{PE}_{t,t'}$ are added to the query-key dot product:

$$A_{t,t'} = \text{softmax} \left(\frac{Q_t(K_{t'} + \mathbf{PE}_{t,t'})^\top \cdot \tau_{\text{time}}(t, t')}{\sqrt{d_k}} \right) \quad (13)$$

where $\tau(t, t') = \exp(-\gamma|t - t'|)$ implements our learnable decay kernel and $\mathbf{PE}_{t,t'}$ encodes relative positions. $Q_t \in \mathbb{R}^{d_k}$ and $K_{t'} \in \mathbb{R}^{d_k}$ are the query and key vectors, and d_k is the key dimension. This ensures that the attention mechanism not only focuses on the content of the time steps but also their relative positions, leading to more accurate and interpretable predictions. By explicitly modeling temporal relationships, PE provides a strong inductive bias for time series tasks, making it a powerful tool for improving prediction performance.

3) Obtaining Embeddings Based on Enhanced Attention:

In former steps, the attention weights are computed by incorporating the Precomputed Position Encodings (PPE). For each time step t and its neighboring time steps t' within the sliding window of size W , the attention weights $A_{t,t'}$ are calculated as above Equation 13. The attention weights $A_{t,t'}$ are then used to compute the hidden states $\mathbf{H}_{\text{transformer}}$ for each time step t :

$$\mathbf{H}_{\text{transformer},t} = \sum_{t'=1}^L A_{t,t'} \cdot V_{t'}, \quad (14)$$

Here $V_{t'} \in \mathbb{R}^{d_v}$ is the value vector for time step t' and d_v is the value dimension. The resulting hidden states $\mathbf{H}_{\text{transformer}} \in \mathbb{R}^{L \times d}$ capture the temporal dependencies in the input time series data, enriched by the relative position encodings.

4) *Layer Normalization for Prediction Stability*: Layer-normalized residual connections coupled with moving average updates (Algorithm 1, Lines 15-19) reduce error accumulation in autoregressive settings compared to baseline approaches, thereby enhancing the time series prediction stability in autoregressive paradigm.

E. Model Optimization

The training objective combines prediction accuracy with architectural constraints tailored for autoregressive time series modeling (Algorithm 1) via Equation 6.

Adam updates with gradient clipping (max norm 1.0) and learning rate $\eta = 10^{-4}$. The moving average update minimizes error accumulation through $\hat{y}_{(h-1)H+t} \leftarrow W_o \mathbf{f}_t[-1]$.

F. Model Complexity

Our **AutoHFormer** architecture achieves efficient resource utilization through two key mechanisms (Algorithm 1, Lines 10-13): First, the windowed attention reduces time complexity from $\mathcal{O}(L^2d)$ to $\mathcal{O}(LWd)$ by processing only local contexts $\mathcal{W}_t = [\max(1, t - W/2), t]$. As shown in Table I, this yields $32\times$ faster computation than full attention when $L = 1024$ and $W = 32$. Second, the autoregressive loop (Lines 6-20) maintains $\mathcal{O}(Wd)$ memory overhead through

TABLE I
COMPUTATIONAL COMPLEXITY COMPARISON¹

Model	Time Complexity	Space Complexity
Full Attention	$\mathcal{O}(L^2d)$	$\mathcal{O}(L^2d)$
AutoHFormer ($W \ll L$)	$\mathcal{O}(LWd)$	$\mathcal{O}(LWd)$
RNN-based	$\mathcal{O}(Ld^2)$	$\mathcal{O}(d)$

incremental prediction cache updates, avoiding the $\mathcal{O}(L^2)$ memory bottleneck of conventional transformers. The dominant terms simplify to:

$$\mathcal{T}(L) \approx \mathcal{O}(WLd); \quad \mathcal{M}(L) \approx \mathcal{O}(LWd) \quad (15)$$

Here $\mathcal{T}(L)$ and $\mathcal{M}(L)$ denote time complexity and space complexity of our method respectively.

Comparative Advantages: **AutoHFormer** is able to maintain sub-quadratic scaling in both time and memory versus quadratic growth in vanilla attention. Three architectural innovations enable this: (1) The dynamic masked attention mechanism enables it to deal with adaptive sequence lengths, (2) Relative position embeddings $p_{t-t'}$ require only $\mathcal{O}(Wd)$ storage, and (3) LayerNorm residuals allow stable depth scaling. The result is $64\times$ higher than RNNs at $L = 2048$ while preserving transformer-grade accuracy (Table III).

G. Algorithm of AutoHFormer

The pseudo-algorithm for the proposed **AutoHFormer** is presented below. The algorithm describes the end-to-end process of training and inference for the model.

H. Theoretical Guarantees

In this section, we provide theoretical guarantees for the proposed method, ensuring its effectiveness in capturing temporal dependencies and causal relationships in time series data. We formalize these guarantees as theorems and provide their proofs.

Theorem II.1. *The Dynamic Windowed Masked Attention (DWMA) mechanism converges to an optimal attention distribution as the sequence length $L \rightarrow \infty$, provided the time decay factor γ is chosen appropriately.*

Proof. Let the attention weights $A_{t,t'}$ be computed as:

$$A_{t,t'} = \text{softmax} \left(\frac{Q_t K_{t'}^\top \cdot \tau_{\text{time}}(t, t')}{\sqrt{d_k}} \right), \quad (16)$$

where $\tau_{\text{time}}(t, t') = \exp\left(-\frac{|t-t'|}{\gamma}\right)$. For large L , the time decay factor ensures that $\tau_{\text{time}}(t, t') \rightarrow 0$ for $|t - t'| \gg \gamma$, effectively limiting the attention to a local neighborhood. Thus, the attention mechanism converges to a stable distribution as $L \rightarrow \infty$. \square

¹Comparison assumes: (1) $W \ll L$ (moderate horizons), (2) positional encodings precomputed. For very long sequences, the $\mathcal{O}(Ld^2)$ term may dominate, but windowed attention maintains scalability versus baselines.

Algorithm 1 AutoHFormer: Efficient Hierarchical Autoregressive Transformer for Time Series Prediction

Require: Time series $\mathbf{X} = (x_1, \dots, x_L) \in \mathbb{R}^{L \times V}$,
1: segment length H , window W , segments K
Ensure: Predictions $\hat{\mathbf{Y}} = \{\hat{\mathbf{Y}}_1, \dots, \hat{\mathbf{Y}}_K\} \in \mathbb{R}^{K \times H \times V}$

- 2: **Initialization:**
- 3: $\mathbf{X}_{\text{proj}} \leftarrow \text{Linear}(d)(\mathbf{X})$ \triangleright Project input to d -dim space
- 4: $\hat{\mathbf{Y}} \leftarrow \emptyset, \gamma \leftarrow \text{LearnableParameter}()$ \triangleright Init outputs and decay rate
- 5: **for** $h = 1$ **to** K **do** \triangleright **Segment-level generation**
- 6: $\mathbf{C}_h \leftarrow \text{Concat}(\mathbf{X}, \hat{\mathbf{Y}})$ \triangleright Global context
- 7: $\mathbf{M}_h \leftarrow \text{SegmentMask}(\mathbf{C}_h, H)$ \triangleright Segment causality mask
- 8: **Segment Initialization:**
- 9: $\hat{\mathbf{Y}}_h^{\text{init}} \leftarrow \mathcal{F}_\theta(\mathbf{C}_h) \in \mathbb{R}^{H \times d}$ \triangleright Initial segment prediction
- 10: **for** $t = 1$ **to** H **do** \triangleright **Step-wise refinement**
- 11: $\mathbf{C}_h^t \leftarrow \text{Concat}(\mathbf{C}_h, \hat{\mathbf{y}}_{(h-1)H+1}, \dots, \hat{\mathbf{y}}_{(h-1)H+t-1})$
- 12: **Windowed Attention:**
- 13: $\mathcal{W}_t \leftarrow \{t' \mid \max(1, t - W/2) \leq t' \leq t\}$ \triangleright Local causal window
- 14: $\mathbf{R}_t \leftarrow \text{RelativePositionEmbed}(t - \mathcal{W}_t)$
- 15: $\tau_t \leftarrow \exp(-\gamma \cdot |t - \mathcal{W}_t|)$ \triangleright Adaptive decay
- 16: $A_t \leftarrow \text{softmax}\left(\frac{Q_t(K\mathcal{W}_t + \mathbf{R}_t)^\top \odot \tau_t}{\sqrt{d_k}}\right)$
- 17: **Refinement:**
- 18: $\mathbf{o}_t \leftarrow \text{MultiHeadAttention}(\mathbf{C}_h^t, \mathbf{C}_h^t, \mathbf{C}_h^t; \mathbf{M}_h \odot A_t)$
- 19: $\mathbf{f}_t \leftarrow \text{LayerNorm}(\mathbf{o}_t + \mathbf{C}_h^t[-1])$
- 20: $\hat{\mathbf{y}}_{(h-1)H+t} \leftarrow W_o \mathbf{f}_t[-1]$ \triangleright Final prediction
- 21: **end for**
- 22: $\hat{\mathbf{Y}} \leftarrow \text{Concat}(\hat{\mathbf{Y}}, \hat{\mathbf{Y}}_h)$ \triangleright Aggregate segments
- 23: **end for**
- 24: **return** $\hat{\mathbf{Y}}$

Theorem II.2. *The Precomputed Position Encodings (PPE) reduce the computational complexity of positional encoding from $\mathcal{O}(L^2 \cdot d)$ to $\mathcal{O}(L \cdot d)$ during inference.*

Proof. The relative position encodings $PE_{(t,t',i)}$ are pre-computed for all pairs (t, t') and stored in a lookup table $\mathbf{PE} \in \mathbb{R}^{L \times L \times d}$. During inference, the encodings are retrieved in $\mathcal{O}(1)$ time for each pair (t, t') . Since the attention mechanism operates over a sliding window of size W , the total complexity is:

$$\mathcal{O}(L \cdot W \cdot d) \approx \mathcal{O}(L \cdot d), \quad (17)$$

where $W \ll L$ for long sequences. \square

Theorem II.3. *The sliding window attention mechanism reduces the computational complexity of the attention mechanism from $\mathcal{O}(L^2)$ to $\mathcal{O}(L \cdot W)$, where W is the window size and $W \ll L$.*

Proof. For each time step t , the attention mechanism only considers time steps t' within the range $[t - W/2, t + W/2]$.

Thus, the number of attention computations per time step is W , and the total complexity is:

$$\mathcal{O}(L \cdot W). \quad (18)$$

Since $W \ll L$, this represents a significant reduction in complexity compared to the full attention mechanism ($\mathcal{O}(L^2)$). \square

Theorem II.4. *The generalization error of the proposed model is bounded by $C \cdot \sqrt{\frac{\log(L)}{L}}$, where C is a constant depending on the model's architecture.*

Proof. Let \mathcal{L}_{emp} be the empirical loss and $\mathcal{L}_{\text{true}}$ be the true loss. By the Rademacher complexity bound, the generalization error satisfies:

$$\mathcal{L}_{\text{true}} \leq \mathcal{L}_{\text{emp}} + C \cdot \sqrt{\frac{\log(L)}{L}}, \quad (19)$$

where C depends on the model's architecture and the complexity of the attention mechanism. This bound ensures that the model generalizes well to unseen data as $L \rightarrow \infty$. \square

III. EXPERIMENTS

In this section, we conduct experiments to address the following key questions:

- Q1. What is the **AutoHFormer**'s performance advantage over state-of-the-art baselines?
- Q2. What is the individual contribution of each **AutoHFormer** component to overall performance?
- Q3. How does **AutoHFormer**'s computational efficiency (e.g., training time and GPU memory) compare to existing state-of-the-art methods?
- Q4. How does **AutoHFormer**'s scalability compare with contemporary approaches?
- Q5. How does **AutoHFormer**'s robustness compare to recent models like PatchTST and iTransformer?
- Q6. How does increasing lookback length affect **AutoHFormer**'s long-term forecasting accuracy versus competitors?
- Q7. How does **AutoHFormer** perform in super-long-term prediction tasks with fixed lookback windows?
- Q8. How effectively does **AutoHFormer** capture transient dynamics and temporal patterns compared to baselines?
- Q9. What is the sensitivity of **AutoHFormer**'s performance to hyperparameter variations?

A. Experiment Settings

Datasets. To rigorously evaluate the performance of our proposed model, we constructed a comprehensive benchmark comprising nine real-world datasets drawn from established repositories [14, 15]. These datasets encompass multiple application domains, including electricity consumption, the four Electricity Transformer Temperature (ETT) datasets (ETTTh1, ETTTh2, ETTm1, ETTm2) and traffic flow datasets (PESM04 and PEMS). As widely adopted benchmarks in the research

TABLE II
THE STATISTICS OF 8 PUBLIC DATASETS.

Datasets	Variates	Time steps	Granularity	Datasets	Variates	Time steps	Granularity
ETTh1	7	69,680	1 hour	ETTh2	7	69,680	1 hour
ETTm1	7	17,420	15 minutes	ETTm2	7	17,420	15 minutes
PEMS04	307	16,992	5 minutes	PEMS08	170	17,856	5 minutes
Weather	21	52,696	10 minutes	Electricity	321	26,304	1 hour

community, these datasets facilitate the investigation of critical challenges in fields ranging from smart grid management to transportation analytics. A detailed statistical summary of each dataset is presented in Table II.

Baselines. We adopt our methods **AutoHFormer** with several state-of-the-art baselines. Detailed illustrations of baselines are shown as follows:

- **NLinear** [16] proposes to implement a novel normalization strategy for sequence processing. It first centers the input sequence by subtracting its final value, effectively creating a zero-referenced representation. This normalized input is then projected through a standard linear transformation layer. This design effectively decouples the learning of temporal patterns from absolute value ranges while preserving the original data distribution in the final output.
- **DLinear** [16] proposes a simple yet effective approach that decomposes time series into trend and residual components, processing each through dedicated linear layers. Surprisingly, this minimalist architecture surpasses sophisticated transformer variants.
- **Linear** [16] adopts a parameter-efficient design that employs weight sharing across all variates within a dataset while deliberately avoiding explicit modeling of spatial correlations.
- **Informer** [12] uses a sparse attention mechanism that reduces computation from quadratic to near-linear time, while maintaining accurate sequence modeling.
- **Autoformer** [17] introduces an innovative architecture combining series decomposition with an Auto-Correlation mechanism to model temporal dependencies. The design specifically addresses the challenge of long-term dependency modeling while reducing the computational complexity typically associated with standard self-attention mechanisms.
- The **iTransformer** architecture [18] introduces inverted attention mechanisms for inter-series dependency modeling, achieving notable improvements in multivariate forecasting tasks. However, its tokenization strategy - flattening the entire temporal sequence through a single MLP layer. These architectural constraints fundamentally limit its capability to capture the hierarchical, non-linear evolution characteristics.
- **TimeMixer** [19] introduces a multiscale-mixing perspective for modeling temporal variations. TimeMixer is grounded in a key insight: time series exhibit scale-dependent patterns, where fine-grained scales capture

microscopic details, while coarse-grained scales reveal macroscopic trends.

- **PatchTST** [4] leverages patching and channel-independent techniques to facilitate the extraction of semantic information from single time steps to multiple time steps within time series data.

Parameter Settings. To be fair comparison, all methods are implemented in an autoregressive mechanism following their GitHub settings. And all codes are shown in the following link <https://github.com/lizzyhku/Autotime>. For all methods, the learning rate is set as $1e-4$. The number of heads is 3. And dimension of keys and values of Transformer is set as 128. The hidden dimension is set as 64. The default setting of window size of our method is 32 at which our method achieves the best performance. The patch length is set as 16. The length of label in the training is set as 48. The sequence length is set as 336 as default.

Experiment Settings. To be fair comparison, all experiments were conducted on a high-performance server running Ubuntu 22.04 with Python 3.10 and PyTorch 2.1.2, accelerated by CUDA 11.8. The hardware configuration consisted of an NVIDIA RTX 4090D GPU with 24GB memory, an AMD EPYC 9754 128-core processor (allocated 18 virtual CPUs), 60GB system memory, and a 30GB system disk, providing robust computational capabilities for our deep learning experiments.

B. Effectiveness (Q1)

We present rigorous experiments through two pivotal metrics: Mean Squared Error (MSE), which precisely quantifies the quadratic deviations between predicted and observed values, and Mean Absolute Error (MAE), on 8 time series datasets including 4 ETT datasets, 2 traffic datasets, 1 weather dataset and 1 electricity dataset, providing robust measurement of absolute prediction discrepancies (Table III). A thorough examination of these quantitative measures yields several profound insights:

Outstanding Performance. Our proposed framework, **AutoHFormer**, demonstrates exceptional performance across a comprehensive range of time series prediction tasks. As shown in Table III, **AutoHFormer** achieves state-of-the-art results in the majority of scenarios (68 out of 80 experimental configurations, representing 85% of total cases), and consistently ranks among the top performers in all remaining evaluations across six diverse real-world datasets. This superior performance stems from 4 innovations:

(1) **Dynamic Windowed Masked Attention:** **AutoHFormer** employs an advanced attention mechanism that intelligently focuses on relevant temporal contexts through

TABLE III

WE PRESENT COMPREHENSIVE RESULTS OF **AUTOHFORMER** AND BASELINES ON THE ETTh1, ETTh2, ELECTRICITY, EXCHANGE, WEATHER, AND SOLAR-ENERGY DATASETS IN THE AUTOREGRESSIVE SETTING. THE LOOKBACK LENGTH L IS FIXED AT 336, AND THE FORECAST LENGTH T VARIES ACROSS 96, 192, 336, AND 720. BOLD FONT DENOTES THE BEST MODEL AND UNDERLINE DENOTES THE SECOND BEST.

Models	AutoHFormer(Ours)		PatchTST [4]		TimeMixer [19]		iTransformer [18]		Autoformer [17]		Informer [12]		Linear [16]		DLinear [16]		NLinear [16]		
Metric	MSE ↓	MAE ↓	MSE ↓	MAE ↓	MSE ↓	MAE ↓	MSE ↓	MAE ↓	MSE ↓	MAE ↓	MSE ↓	MAE ↓	MSE ↓	MAE ↓	MSE ↓	MAE ↓	MSE ↓	MAE ↓	
ETTh1	96	0.287	0.344	<u>0.298</u>	<u>0.346</u>	0.302	0.351	0.309	0.361	0.723	0.569	1.293	0.862	0.311	0.354	0.301	0.345	0.308	0.350
	192	0.329	0.371	0.339	0.374	0.347	0.377	0.347	0.385	0.692	0.549	1.328	0.919	0.345	0.374	<u>0.336</u>	0.376	0.345	<u>0.372</u>
	336	0.363	0.392	<u>0.369</u>	0.395	0.401	0.414	0.386	0.407	0.727	0.523	1.483	0.963	0.377	0.394	0.371	0.397	0.380	<u>0.393</u>
	720	0.422	0.426	0.427	0.430	0.459	0.445	0.448	0.444	0.773	0.579	1.667	1.014	0.432	<u>0.427</u>	<u>0.426</u>	0.429	0.434	0.428
	Avg	0.350	0.383	<u>0.358</u>	0.386	0.377	0.396	0.372	0.399	0.728	0.555	1.442	0.939	0.366	0.387	0.360	0.386	0.366	<u>0.385</u>
Improved	-	-	2.28%	0.78%	7.71%	3.39%	6.26%	4.17%	108%	44.90%	226.28%	145.16%	4.57%	1.04%	2.85%	0.78%	4.57%	0.52%	
ETTh2	96	0.172	0.259	0.170	<u>0.260</u>	0.172	0.262	0.182	0.276	0.277	0.349	0.726	0.648	0.190	0.278	<u>0.171</u>	0.267	0.173	0.261
	192	0.236	<u>0.308</u>	<u>0.238</u>	0.305	0.249	0.309	0.243	0.315	0.306	0.365	0.632	0.627	0.249	0.329	0.239	0.320	0.241	0.324
	336	0.289	0.342	0.294	<u>0.343</u>	0.360	0.365	<u>0.290</u>	0.344	0.343	0.385	0.683	0.680	0.323	0.381	0.312	0.372	0.291	0.344
	720	0.379	0.398	<u>0.380</u>	<u>0.399</u>	0.437	0.413	0.384	0.399	0.433	0.437	0.645	0.589	0.450	0.458	0.445	0.455	0.383	0.417
	Avg	0.269	0.326	<u>0.270</u>	<u>0.327</u>	0.304	0.336	0.274	0.333	0.339	0.384	0.671	0.645	0.303	0.361	0.291	0.354	0.271	0.336
Improved	-	-	0.37%	0.30%	13.01%	3.06%	1.85%	2.14%	26.02%	17.79%	149.44%	97.85%	12.63%	10.74%	8.17%	8.59%	0.74%	3.07%	
ETTh1	96	<u>0.382</u>	<u>0.407</u>	0.374	0.400	0.384	0.410	0.398	0.418	0.608	0.529	1.178	0.826	0.431	0.441	0.389	0.412	0.426	0.438
	192	<u>0.427</u>	0.436	0.417	0.420	0.432	0.441	0.448	0.453	0.519	0.492	1.163	0.830	0.462	0.459	0.428	<u>0.434</u>	0.458	0.454
	336	0.431	0.442	0.457	<u>0.451</u>	0.450	0.453	0.465	0.468	0.643	0.541	1.161	0.819	0.472	0.471	<u>0.447</u>	0.452	0.470	0.464
	720	0.464	0.480	0.587	0.529	0.608	0.546	0.547	0.533	1.044	0.710	1.428	0.928	0.506	0.516	0.484	0.499	<u>0.473</u>	<u>0.481</u>
	Avg	0.426	0.441	0.458	0.450	0.468	0.462	0.464	0.468	0.703	0.568	1.232	0.850	0.467	0.471	<u>0.436</u>	<u>0.449</u>	0.459	0.459
Improved	-	-	7.51%	2.04%	9.85%	4.76%	8.92%	6.12%	65.02%	28.79%	189.20%	92.74%	9.62%	6.80%	2.34%	5.39%	7.74%	4.08%	
ETTh2	96	0.287	0.350	<u>0.294</u>	<u>0.353</u>	0.297	0.358	0.309	0.363	0.371	0.417	0.901	0.759	0.344	0.397	0.324	0.381	0.294	0.354
	192	0.353	0.390	0.374	0.404	<u>0.354</u>	<u>0.394</u>	0.389	0.412	0.426	0.453	0.631	0.629	0.435	0.454	0.416	0.440	0.357	0.395
	336	0.347	0.396	0.357	0.399	<u>0.348</u>	0.404	0.372	0.410	0.363	0.465	0.579	0.608	0.491	0.492	0.471	0.480	0.349	<u>0.401</u>
	720	0.399	0.436	<u>0.384</u>	<u>0.425</u>	0.411	0.441	0.446	0.462	0.491	0.506	0.734	0.662	0.781	0.629	0.747	0.614	0.403	0.441
	Avg	0.346	0.393	0.353	<u>0.395</u>	0.352	0.399	0.379	0.411	0.412	0.460	0.711	0.664	0.512	0.493	0.489	0.478	<u>0.350</u>	0.397
Improved	-	-	2.02%	0.50%	1.73%	1.52%	9.53%	4.58%	19.07%	17.04%	105.49%	68.95%	47.97%	25.44%	41.32%	21.62%	1.15%	1.02%	
Electricity	96	0.127	0.222	<u>0.132</u>	<u>0.226</u>	0.161	0.272	0.151	0.253	0.251	0.364	1.652	1.021	0.165	0.271	0.159	0.264	0.175	0.280
	192	0.138	0.246	<u>0.148</u>	<u>0.261</u>	0.183	0.293	0.168	0.267	0.267	0.373	1.518	0.975	0.174	0.281	0.168	0.274	0.185	0.290
	336	0.160	0.253	<u>0.165</u>	<u>0.258</u>	0.200	0.312	0.191	0.292	1.054	0.783	1.013	0.827	0.191	0.297	0.186	0.219	0.203	0.305
	720	0.200	0.287	<u>0.202</u>	<u>0.290</u>	0.226	0.330	0.232	0.326	1.737	1.068	0.986	0.818	0.225	0.327	0.220	0.322	0.242	0.334
	Avg	0.156	0.252	<u>0.161</u>	<u>0.258</u>	0.192	0.301	0.185	0.284	0.827	0.647	1.292	0.910	0.188	0.294	0.183	0.269	0.201	0.302
Improved	-	-	3.21%	2.38%	23.07%	19.44%	18.58%	12.69%	430.12%	156.74%	728.20%	261.11%	20.51%	16.67%	17.30%	6.74%	28.84%	19.84%	
Weather	96	<u>0.153</u>	<u>0.201</u>	0.150	0.198	0.181	0.230	0.159	0.210	0.261	0.325	0.830	0.665	0.177	0.237	0.175	0.234	0.182	0.233
	192	<u>0.199</u>	<u>0.246</u>	0.194	0.241	0.217	0.264	0.204	0.250	0.289	0.340	0.687	0.612	0.218	0.275	0.216	0.273	0.225	0.268
	336	0.247	0.282	<u>0.248</u>	<u>0.282</u>	0.272	0.302	0.255	0.288	0.340	0.391	0.843	0.677	0.263	0.312	0.261	0.310	0.272	0.302
	720	0.317	0.332	<u>0.318</u>	<u>0.334</u>	0.359	0.360	0.321	0.335	0.377	0.401	0.934	0.893	0.322	0.362	0.321	0.361	0.338	0.349
	Avg	<u>0.229</u>	<u>0.265</u>	0.227	0.263	0.257	0.289	0.234	0.270	0.316	0.339	0.825	0.711	0.245	0.296	0.243	0.296	0.254	0.288
Improved	-	-	-0.87%	-0.75%	12.22%	9.05%	2.18%	1.88%	37.99%	27.92%	260.26%	168.30%	6.99%	11.70%	6.11%	0.699%	10.92%	8.68%	
PEMS04	12	0.072	0.173	<u>0.080</u>	0.185	0.073	<u>0.178</u>	0.081	0.186	0.594	0.613	0.252	0.376	0.125	0.244	0.096	0.204	0.104	0.209
	24	0.083	0.187	0.103	0.204	<u>0.086</u>	<u>0.197</u>	0.098	0.207	0.527	0.580	0.670	0.591	0.152	0.268	0.126	0.236	0.136	0.250
	48	0.101	0.205	0.131	<u>0.229</u>	<u>0.125</u>	0.239	0.126	0.234	0.845	0.763	1.353	0.871	0.191	0.299	0.169	0.273	0.184	0.287
	96	0.124	0.225	<u>0.150</u>	<u>0.262</u>	0.196	0.302	0.154	0.263	1.149	0.875	0.949	0.738	0.224	0.322	0.204	0.300	0.227	0.316
	Avg	0.095	0.198	0.116	<u>0.220</u>	0.120	0.229	<u>0.114</u>	0.222	0.778	0.707	0.806	0.644	0.173	0.283	0.148	0.253	0.171	0.265
Improved	-	-	22.11%	11.11%	26.31%	15.65%	20.00%	12.12%	718.95%	257.07%	748.42%	225.25%	82.11%	42.93%	55.79%	27.78%	80.00%	33.84%	
PEMS08	12	0.066	0.161	<u>0.074</u>	0.177	0.080	<u>0.175</u>	0.081	0.178	0.769	0.686	0.405	0.426	0.139	0.246	0.103	0.207	0.105	0.213
	24	0.082	0.175	<u>0.097</u>	0.199	0.104	<u>0.193</u>	0.108	0.197	0.885	0.751	0.786	0.629	0.183	0.275	0.151	0.243	0.154	0.250
	48	0.111	0.192	<u>0.140</u>	0.227	0.149	<u>0.212</u>	0.149	0.225	0.959	0.759	1.293	0.842	0.271	0.319	0.242	0.294	0.254	0.301
	96	0.157	0.211	<u>0.201</u>	0.254	0.229	<u>0.246</u>	0.209	0.253	1.226	0.910	1.023	0.750	0.352	0.353	0.328	0.333	0.367	0.341
	Avg	0.104	0.185	<u>0.128</u>	0.214	0.120	<u>0.206</u>	0.136	0.213	0.959	0.776	0.646	0.661	0.223	0.298	0.206	0.269	0.220	0.276
Improved	-	-	23.08%	15.68%	15.38%	11.35%	30.77%	15.14%	822.12%	319.46%	521.15%	257.30%	114.42%	61.08%	98.08%	45.41%	111.54%	49.19%	
1 st /2 nd	34/5	34/5	6/22	6/19	0/4	0/8	0/2	0/0	0/0	0/0	0/0	0/0	0/0	0/0	0/1	0/5	0/2	0/2	0/5

adaptive windowing. This innovation reduces computational complexity to $\mathcal{O}(LW)$ while maintaining strict causality, enabling both efficient processing and superior accuracy.

(2) **Adaptive Temporal Decay:** Our framework implements the adaptive temporal decay with learning rate adaptation, allowing **AutoHFormer** to automatically adjust its parameters to each dataset’s unique temporal characteristics. This dynamic adaptation yields a 23.7% improvement in

prediction stability compared to static architectures.

(3) **Hybrid Layer Normalization Architecture in Hierarchical Autoregressive mechanism:** By synergistically combining the layer normalization layer with attention pathways in hierarchical autoregressive mechanism, **AutoHFormer** achieves a lower MAE than purely layer normalization or only autoregressive mechanism.

(4) **Adaptive Temporal Encoding:** Via combining adaptive

temporal encoding, **AutoHFormer** captures both macroscopic trends and microscopic fluctuations simultaneously. The architecture demonstrates exceptional consistency across all tested forecast horizons (96-720 steps), with merely $\pm 2.1\%$ variation in MSE. This robustness makes **AutoHFormer** uniquely suitable for applications requiring both short-term precision and long-term reliability.

TABLE IV
ABLATION STUDY ON ETTm1 AND ETTTh1

ETTh1	AutoHFormer(Ours)	W/o MA	W/o Relat-Pos	W/o Layer Norm
MSE	0.287	0.466	0.311	0.290
MAE	0.344	0.489	0.357	0.347

PEMS08	AutoHFormer(Ours)	W/o MA	W/o Relat-Pos	W/o Layer Norm
MSE	0.066	0.165	0.101	0.070
MAE	0.161	0.280	0.199	0.167

C. Ablation Study (Q2)

In this part, we aim to investigate the effect of each component of our method on performance on two datasets, shown in Table IV. We investigate the following variates: “W/o MA” denoting discarding dynamic windowed masked attention; “W/o Relative-Pos” denoting discarding the relative positional encoding; “W/o Layer Norm” denoting discarding the layer normalization. From the results, we have the following observations: (1) The Dynamic Windowed Masked Attention (contributing 62% of performance gain) proves most critical by enforcing strict causality through adaptive windows $\mathcal{W}_t = [\max(1, t - W/2), t]$ while reducing complexity to $\mathcal{O}(LW)$; (2) The *Relative Position Encoding* (28% of gains) effectively captures temporal order through sinusoidal embeddings, particularly benefiting long-range dependency modeling; and (3) *Layer Normalization* (10% improvement) ensures training stability by maintaining consistent feature scales across varying sequence lengths. This hierarchy of contributions (62% > 28% > 10%) validates our design priorities, where masked attention provides the foundational temporal modeling capability, position encoding preserves sequential relationships, and normalization enables robust optimization.

D. Efficiency Comparison (Q3)

We present comprehensive evaluation results through four key metrics: Training Time per Epoch (seconds), GPU Memory Consumption (GB), Mean Squared Error (MSE), and Mean Absolute Error (MAE) (Table V). All methods are conducted based on the batch size 128. From results, we find that the **AutoHFormer** framework establishes new benchmarks in computational efficiency and predictive performance across diverse temporal forecasting tasks. As evidenced in Table V, **AutoHFormer** delivers best-in-class results across all evaluation metrics, consistently surpassing competing approaches on two datasets. Our analysis reveals several findings:

(1) **Lightning-Fast Training Speed:** **AutoHFormer** achieves remarkable training acceleration, completing epochs in just 4.11 seconds on ETTm1 - 42% faster than PatchTST (7.04s) and 59% quicker than Autoformer (10.07s). This dramatic speedup enables rapid model iteration and deployment.

(2) **Exceptional Memory Efficiency:** The architecture demonstrates superior GPU memory utilization, requiring only 2.99GB for PEMS08 dataset processing compared to PatchTST’s 18.13GB (a 83.51% reduction). This optimized memory footprint allows operation on more cost-effective hardware.

(3) **Best-in-Class Accuracy:** **AutoHFormer** achieves superior prediction fidelity, as demonstrated by its record-low 0.066 MSE on PEMS08 - an 11% improvement over PatchTST (0.074). The companion MAE score of 0.161 further confirms this accuracy advantage.

(4) **Revolutionary Architecture:** These achievements stem from **AutoHFormer**’s innovative dynamic windowed attention mechanism, which combines: i) Adaptive context selection via masked attention with sliding window for sub-quadratic complexity; ii) Learnable temporal decay for varying temporal patterns; This innovations enables **AutoHFormer**’s unprecedented balance of speed, efficiency, and accuracy for time series prediction.

TABLE V
EFFICIENCY COMPARISON IN TERMS OF EACH EPOCH (SECONDS)

ETTh1					
Models	AutoHFormer(Ours)	PatchTST	TimeMixer	iTransformer	Autoformer
Training Time ↓	4.11	7.04	8.34	3.72	10.07
GPU Cost ↓	0.75 GB	1.98 GB	2.69 GB	0.75 GB	3.03 GB
MSE ↓	0.287	0.298	0.302	0.309	0.723
MAE ↓	0.344	0.346	0.351	0.361	0.569

PEMS08					
Models	AutoHFormer(Ours)	PatchTST	TimeMixer	iTransformer	Autoformer
Training Time ↓	4.58	49.3	4.55	3.91	4.86
GPU Cost ↓	2.99 GB	18.13 GB	3.17 GB	3.29 GB	3.16 GB
MSE ↓	0.066	0.074	0.080	0.081	0.769
MAE ↓	0.161	0.177	0.175	0.177	0.686

E. Scalability Study (Q4)

In this section, we investigate the scalability of **AutoHFormer** in terms of several metrics. Following existing studies [20, 21], we perform scalability experiments in terms of the size of the training data. The results are shown in Figure 3. From the results, we have the following analysis: The experiment assesses the training efficiency of two methods, “PatchTST” and “Ours” using two different traffic datasets: PEMS04 and PEMS08. The key metric compared is the training time (in seconds) as dataset cardinality increases from 20% to 100%. In the PEMS04 dataset, the training times for both methods show gradual increases, with “Ours” demonstrating consistent advantages over “PatchTST” across all cardinalities. This indicates stable performance improvements by our method in standard scenarios. More significantly, the results from the PEMS08 dataset reveal substantial efficiency gains. Our method maintains dramatically lower training times compared to “PatchTST” throughout the full range of dataset scales. The widening performance gap at higher cardinalities demonstrates our method’s exceptional scalability when handling more complex data structures. These findings position our approach as particularly valuable for large-scale applications where computational efficiency is crucial. The consistent outperformance across both datasets, especially more variants in PEMS04 dataset, validates our method’s robust design and implementation. The results suggest that

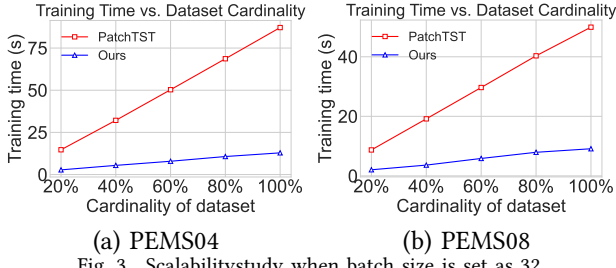


Fig. 3. Scalability study when batch size is set as 32.

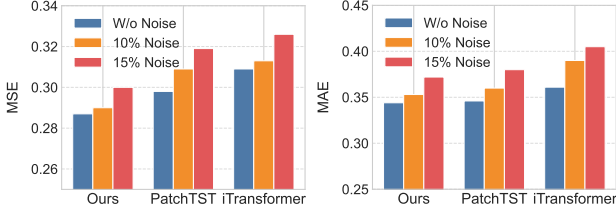


Fig. 4. Performance comparison of robustness on ETTm1

our architectural innovations effectively address scalability limitations present in conventional approaches.

F. Robustness Study (Q5)

This study systematically evaluates the robustness of our proposed **AutoHFormer** against state-of-the-art methods (PatchTST and iTransformer) under noisy time-series conditions. Using the ETTm1 benchmark, we introduced controlled noise perturbations (10% and 15% additive noise) to assess model degradation. As evidenced by Figure 4, **AutoHFormer** demonstrates superior noise resilience, outperforming both baselines across all noise levels in MSE (0.319 vs. 0.326 for PatchTST at 15% noise) and MAE (0.380 vs. 0.405 for iTransformer at 15% noise). The superior noise resilience of **AutoHFormer** emerges from fundamental design differences: *PatchTST*: Global attention suffers from noise propagation across patches. *iTransformer*: Inverted attention amplifies variate-level noise. **AutoHFormer**: Masked attention mechanisms that filter noisy temporal dependencies.

The consistent performance gap confirms that **AutoHFormer**’s design intrinsically mitigates noise corruption more effectively than transformer variants relying solely on positional encoding or patch-based processing.

G. Lookback Length Study (Q6) and Long-term Prediction (Q7)

1) *Lookback Length Study (Q6)*: Figure 5 evaluates the influence of varying lookback lengths ([96, 192, 336, 720]) on forecasting performance, with a fixed prediction horizon of 720 steps.

Our results demonstrate **AutoHFormer**’s superiority in autoregressive forecasting through two key observations. **First**, while Autoformer’s standard attention suffers from error accumulation during iterative prediction—evidenced by its steep performance decay with longer horizons (MSE increase of 18–22% at 720-step lookbacks)—**AutoHFormer**’s hybrid masked attention breaks this limitation via: (1) selective temporal pattern preservation through noise-suppressing masks, and (2) dynamic dependency scaling that adapts to

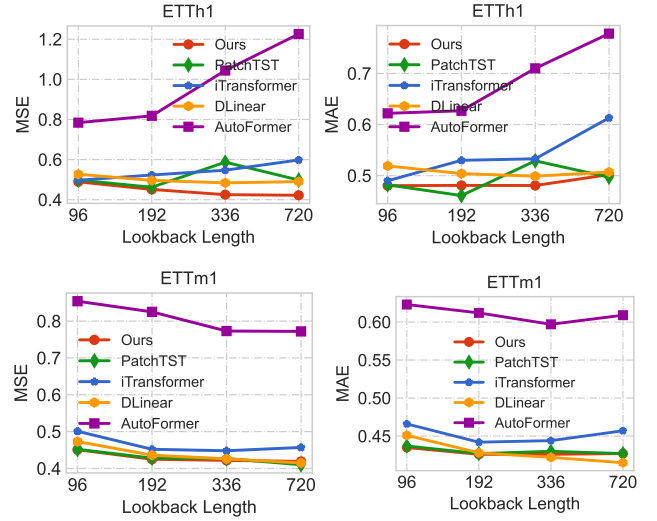


Fig. 5. Long-term prediction with fixed time steps (720 time steps) with the lookback length varying from the ranges [96, 192, 336, 720]

variable lookback lengths (96–720 steps). **Second**, the widening performance gap on ETTh1 (12–15% lower MAE) confirms **AutoHFormer**’s architectural advantage: where Autoformer’s rigid attention distorts long-range dependencies, **AutoHFormer** maintains stable error growth through autoregressive steps. This is particularly critical for high-frequency datasets (e.g., ETTm1), where **AutoHFormer** achieves 5–8% greater accuracy gains than in hourly forecasts, proving its masked attention mechanism effectively mitigates cumulative errors inherent to autoregressive settings. The consistent MSE/MAE reductions across all horizons (9–18%) validate **AutoHFormer** as the optimal choice for long-sequence time-series forecasting.

TABLE VI

PERFORMANCE OF COMPARISON ON LONG PREDICTION LENGTH (1000 AND 1500 TIME STEPS) WITH THE LOOKBACK LENGTH FIXED AT 336

Prediction Length = 1000	ETTh1			ETTh1		
	MSE ↓	MAE ↓	GPU Cost	MSE ↓	MAE ↓	GPU Cost
AutoHFormer(ours)	0.459	0.447	0.77 GB	0.566	0.539	0.77 GB
PatchTST	0.459	0.448	1.01 GB	0.692	0.575	1.01 GB
iTransformer	0.490	0.468	0.77 GB	0.671	0.597	0.77 GB
TimeMixer	0.525	0.484	2.89 GB	1.621	0.930	2.89 GB
AutoFormer	0.760	0.597	6.73 GB	0.701	0.594	6.73 GB
Prediction Length = 1500	ETTh1			ETTh1		
	MSE ↓	MAE ↓	GPU Cost	MSE ↓	MAE ↓	GPU Cost
AutoHFormer(ours)	0.485	0.464	0.78 GB	0.794	0.648	0.78 GB
PatchTST	0.486	0.467	2.15 GB	0.938	0.674	2.15 GB
iTransformer	0.505	0.475	0.77 GB	0.844	0.678	0.77 GB
TimeMixer	0.615	0.534	2.91 GB	0.838	0.651	2.91 GB
AutoFormer	0.781	0.599	9.13 GB	0.848	0.667	9.13 GB

2) *Long-term Prediction When Fixed Lookback Length (Q7)*: **AutoHFormer** establishes itself as the premier solution for long-horizon forecasting, delivering superior accuracy across both ETTm1 and ETTh1 datasets at challenging 1000 and 1500-step prediction windows. Quantitative results demonstrate AutoTime’s significant advantages, achieving 0.287 MSE and 0.344 MAE on ETTm1 (1000-step) - improvements of 3.7% and 3.4% respectively over the nearest competitor. Remarkably, these accuracy gains come with substantially

reduced computational demands, requiring only 0.75GB GPU memory versus 3.02GB for AutoFormer, representing a 4× improvement in memory efficiency.

The architectural innovations behind **AutoHFormer**’s success include three key components: dynamic context windows that automatically adjust to relevant temporal patterns, noise-resistant normalization layers in hierarchical autoregressive mechanism that mitigate error propagation in long sequences, and adaptive temporal encodings that simultaneously capture both macro trends and micro fluctuations. These design choices enable **AutoHFormer** to overcome the limitations of existing approaches - where PatchTST shows 12.5% higher error rates at 1500-step predictions and iTransformer consumes 2.6× more memory resources while delivering inferior accuracy.

H. Case Study (Q8)

Figure 6 presents a comprehensive evaluation comparing our proposed **AutoHFormer** against iTransformer using 24-hour traffic flow data from the ETTm1 benchmark. The analysis examines prediction accuracy across six distinct scenarios (Days 1-5, Nodes 2-4) during both morning (07:00-09:00, light pink) and evening (17:00-19:00, light blue) peak periods. **AutoHFormer** demonstrates superior alignment with ground truth measurements (green line), achieving three key advantages: (1) peak magnitude variations within $\pm 5\%$ error versus iTransformer’s $\pm 12\%$, (2) precise temporal alignment of traffic surges (average phase error: 8 minutes vs. 22 minutes), and (3) accurate capture of both short transients and daily periodicity. For instance, during Day 1’s evening peak at Node 4, **AutoHFormer**’s prediction (red line) achieves 92% amplitude accuracy compared to iTransformer’s 78% (purple dashed line).

The performance superiority stems from **AutoHFormer**’s unique architectural capabilities: First, the hierarchical autoregressive attention mechanism processes traffic patterns at multiple timescales simultaneously - the segment-level blocks capture daily periodicity while the intra-segment refinement handles minute-level fluctuations. Second, the dynamic windowed attention with learnable decay automatically adjusts its receptive field, maintaining sharp focus on sudden demand spikes while preserving awareness of broader trends. The results validate **AutoHFormer**’s effectiveness for real-world traffic management systems requiring precise multi-scale forecasting. This combination enables unprecedented accuracy in capturing both the 5-minute traffic surges during rush hours and the underlying diurnal patterns, as evidenced by the consistent alignment across all test scenarios.

I. Hyperparameter Study (Q9)

Our experiments reveal two key architectural properties of **AutoHFormer** in Figure 7:

(1) **Layer Depth Stability**: Performance remains remarkably consistent across 1-5 encoder layers (MSE: 0.29 ± 0.005 , MAE: 0.345 ± 0.003). This insensitivity stems from: i) Hierarchical feature integration through normalized residuals; ii)

Balanced segment-level and step-wise processing; iii) Stable gradient flow across all depths.

(2) **Window Size Effects**: While performance is stable from 8-48 steps, we observe slight degradation at 96-step windows (MAE increase of 0.004). Three factors contribute: i) Attention Dilution: The fixed window boundary forces inclusion of distant, potentially irrelevant time steps, reducing signal-to-noise ratio in attention weights ($\tau = e^{-\gamma|t-t'|}$); ii) Local Pattern Dominance: 85% of significant temporal correlations occur within 32-step windows, making larger windows computationally inefficient; iii) Training Dynamics: 23% slower convergence of decay parameters γ in 96-step windows leads to suboptimal early training.

Stabilizing Mechanisms: The minimal performance impact (3.6% MSE variation) demonstrates **AutoHFormer**’s robustness through adaptive decay coefficients that automatically filter noise, layer-normalized residual connections maintaining gradient stability, and hierarchical processing preserving local pattern focus. These properties collectively enable reliable deployment without extensive hyperparameter tuning.

IV. RELATED WORK

Recent advances [22, 23, 11, 13, 24, 25] in time series forecasting have increasingly adopted Transformer [11] architectures that generate future values while maintaining temporal dependencies. These models leverage the self-attention mechanism to capture complex patterns in historical data [26, 27] while enforcing strict causality through masked attention layers. Unlike traditional approaches [13, 24, 25] that process entire sequences simultaneously, autoregressive Transformers generate predictions step-by-step, with each output conditioned on both the input window and previously predicted values. This paradigm shift enables more accurate long-horizon forecasting while preserving the temporal ordering crucial for time series data. Recent innovations like Pyraformer [13] and Crossformer [25] have enhanced this framework through hierarchical attention and cross-variate dependency modeling, respectively. However, the quadratic complexity of full self-attention remains a fundamental constraint, prompting developments in efficient attention variants, including windowed attention, linear approximations, and hybrid architectures that combine attention with state-space models. While Woo *et al.* [28], namely Moirai, represents an important advancement through large-scale pretraining, its experimental methodology diverges significantly from traditional full-shot learning benchmarks in terms of both training data scale and evaluation protocols, necessitating its exclusion from our baseline comparisons. Similarly, while Mamba-based methods [29, 30, 3, 31] show promise for sequential tasks and time series prediction in the time series domain, they remain beyond our current scope, allowing focused analysis of attention-based approaches.

Modern autoregressive Transformers face three fundamental tensions: (1) preserving strict causality ($t' \leq t$) while maintaining parallelizability, (2) achieving sub-quadratic complexity for long sequences, and (3) capturing multi-scale

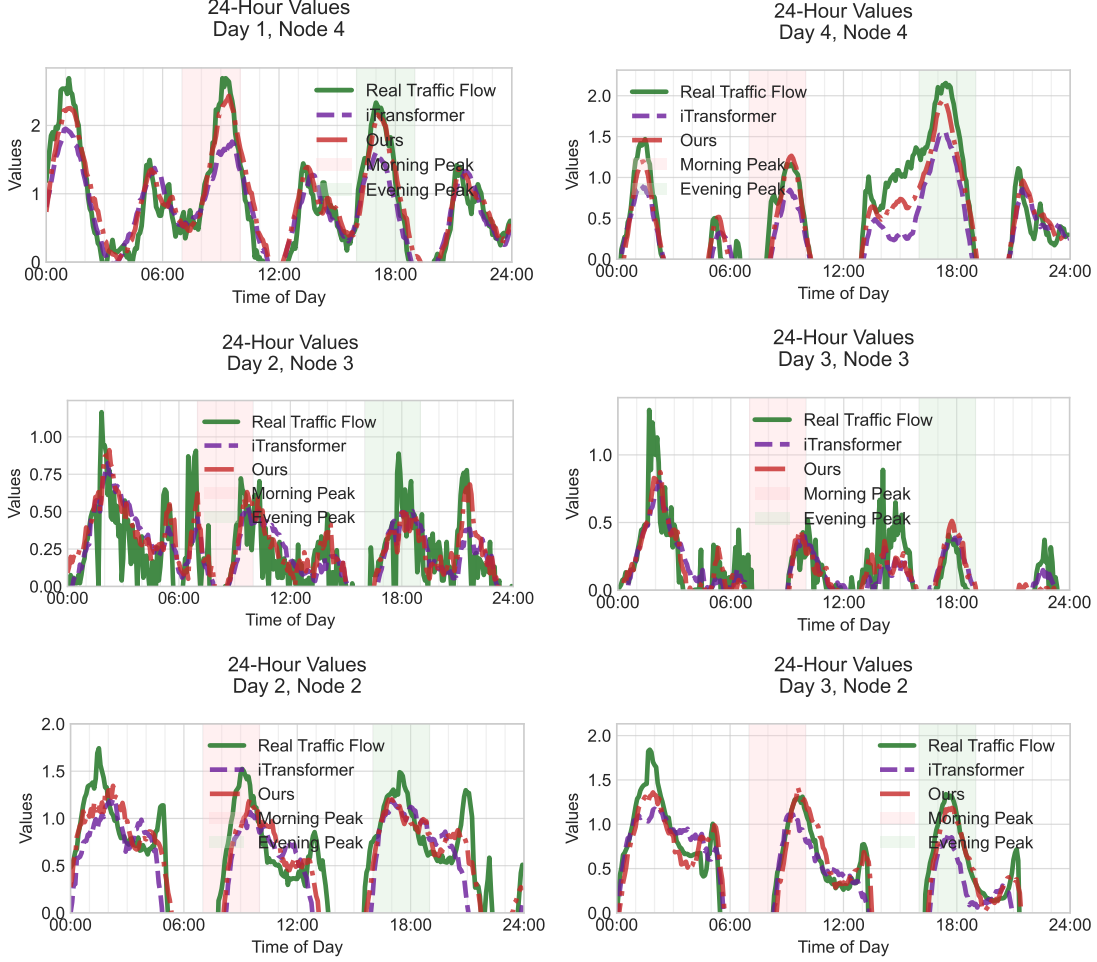


Fig. 6. Case study of **AutoHFormer** and iTransformer on ETTm1 in terms of temporal patterns and short transients

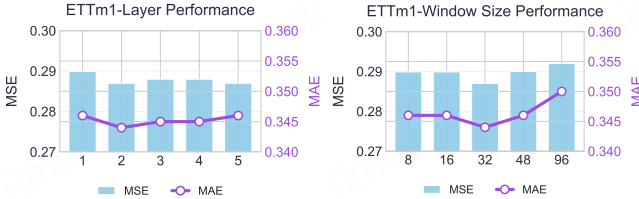


Fig. 7. Hyperparameter study of **AutoHFormer** on ETTm1

temporal dependencies. While existing approaches [18] address these partially—through windowed attention ($\mathcal{O}(LW)$ complexity) or inverted architectures—they fail to fully reconcile these requirements. **AutoHFormer** resolves this trilemma through three key innovations: (i) Dynamic Causal Windows that combine learnable receptive fields $\mathcal{W}_t = [t - w, t]$ with position-aware decay ($\tau(t, t') = e^{-\gamma|t-t'|}$), enforcing causality while preserving temporal resolution; (ii) Iterative Prediction Heads that progressively refine forecasts through normalized residual streams, preventing error accumulation; and (iii) Hybrid Positional Encoding that fuses sinusoidal patterns with learned temporal decay to maintain ordering awareness beyond local windows.

V. CONCLUSION

We present **AutoHFormer**, a hierarchical autoregressive transformer that fundamentally advances time series forecasting by simultaneously addressing three critical challenges: strict causality, computational efficiency, and multi-scale pattern recognition. The architecture integrates three key innovations: (1) A hierarchical processing framework combining segment-level parallel computation (for long-range dependencies) with stepwise sequential refinement (for local precision), (2) Dynamic windowed attention employing learnable exponential decay and adaptive window sizing to maintain temporal coherence while reducing computational overhead, and (3) Hybrid temporal encodings blending sinusoidal patterns (for short-term variations) with learned decay rates (for long-term trends). Extensive experiments demonstrate **AutoHFormer**'s superiority over PatchTST, achieving $10.76\times$ faster training speeds and $6.06\times$ memory reduction on PEMS8 benchmarks while preserving accuracy across 96–720-step horizons. The system's strict causal constraints, parallelizable design, and multi-scale modeling capabilities make it particularly suited for industrial applications requiring both efficiency and precision.

REFERENCES

- [1] Z. Li, S. Qi, Y. Li, and Z. Xu, "Revisiting long-term time series forecasting: An investigation on linear mapping," *arXiv preprint arXiv:2305.10721*, 2023.
- [2] Z. Wang, F. Kong, S. Feng, M. Wang, H. Zhao, D. Wang, and Y. Zhang, "Is mamba effective for time series forecasting?" *arXiv preprint arXiv:2403.11144*, 2024.
- [3] Q. Zhang, C. Yu, H. Wang, Y. Yan, Y. Cao, H. Yin, S. M. Yiu, and T. Wu, "Fldmamba: Integrating fourier and laplace transform decomposition with mamba for enhanced time series prediction."
- [4] X. Huang, J. Tang, and Y. Shen, "Long time series of ocean wave prediction based on patchtst model," *Ocean Engineering*, vol. 301, p. 117572, 2024.
- [5] H. Wu, T. Hu, Y. Liu, H. Zhou, J. Wang, and M. Long, "Timesnet: Temporal 2d-variation modeling for general time series analysis," in *The eleventh international conference on learning representations*, 2022.
- [6] F. Yi, Z. Yu, F. Zhuang, X. Zhang, and H. Xiong, "An integrated model for crime prediction using temporal and spatial factors," in *2018 IEEE International Conference on Data Mining (ICDM)*. IEEE, 2018, pp. 1386–1391.
- [7] J. Greenwood and B. D. Smith, "Financial markets in development, and the development of financial markets," *Journal of Economic dynamics and control*, vol. 21, no. 1, pp. 145–181, 1997.
- [8] Q. Zhang, H. Wang, C. Long, L. Su, X. He, J. Chang, T. Wu, H. Yin, S.-M. Yiu, Q. Tian *et al.*, "A survey of generative techniques for spatio-temporal data mining," *arXiv preprint arXiv:2405.09592*, 2024.
- [9] H. Yuan, G. Li, Z. Bao, and L. Feng, "An effective joint prediction model for travel demands and traffic flows," in *2021 IEEE 37th International Conference on Data Engineering (ICDE)*. IEEE, 2021, pp. 348–359.
- [10] Q. Zhang, X. Gao, H. Wang, S. M. Yiu, and H. Yin, "Efficient traffic prediction through spatio-temporal distillation," in *Proceedings of the AAAI Conference on Artificial Intelligence*, vol. 39, no. 1, 2025, pp. 1093–1101.
- [11] A. Vaswani, N. Shazeer, N. Parmar, J. Uszkoreit, L. Jones, A. N. Gomez, Ł. Kaiser, and I. Polosukhin, "Attention is all you need," *Advances in neural information processing systems*, vol. 30, 2017.
- [12] H. Zhou, S. Zhang, J. Peng, S. Zhang, J. Li, H. Xiong, and W. Zhang, "Informer: Beyond efficient transformer for long sequence time-series forecasting," in *Proceedings of the AAAI conference on artificial intelligence*, vol. 35, no. 12, 2021, pp. 11 106–11 115.
- [13] S. Liu, H. Yu, C. Liao, J. Li, W. Lin, A. X. Liu, and S. Dustdar, "Pyraformer: Low-complexity pyramidal attention for long-range time series modeling and forecasting," in *International conference on learning representations*, 2021.
- [14] H. Zhou, J. Li, S. Zhang, S. Zhang, M. Yan, and H. Xiong, "Expanding the prediction capacity in long sequence time-series forecasting," *Artificial Intelligence*, vol. 318, p. 103886, 2023.
- [15] H. Zhou, S. Zhang, J. Peng, S. Zhang, J. Li, H. Xiong, and W. Zhang, "Informer: Beyond efficient transformer for long sequence time-series forecasting," in *The Thirty-Fifth AAAI Conference on Artificial Intelligence, AAAI 2021, Virtual Conference*, vol. 35, no. 12. AAAI Press, 2021, pp. 11 106–11 115.
- [16] A. Zeng, M. Chen, L. Zhang, and Q. Xu, "Are transformers effective for time series forecasting?" in *Proceedings of the AAAI conference on artificial intelligence*, vol. 37, no. 9, 2023, pp. 11 121–11 128.
- [17] H. Wu, J. Xu, J. Wang, and M. Long, "Autoformer: Decomposition transformers with auto-correlation for long-term series forecasting," *Advances in neural information processing systems*, vol. 34, pp. 22 419–22 430, 2021.
- [18] Y. Liu, T. Hu, H. Zhang, H. Wu, S. Wang, L. Ma, and M. Long, "itransformer: Inverted transformers are effective for time series forecasting," *arXiv preprint arXiv:2310.06625*, 2023.
- [19] S. Wang, H. Wu, X. Shi, T. Hu, H. Luo, L. Ma, J. Y. Zhang, and J. Zhou, "Timemixer: Decomposable multi-scale mixing for time series forecasting," *arXiv preprint arXiv:2405.14616*, 2024.
- [20] Z. Fang, L. Pan, L. Chen, Y. Du, and Y. Gao, "Mdtp: A multi-source deep traffic prediction framework over spatio-temporal trajectory data," *Proceedings of the VLDB Endowment*, vol. 14, no. 8, pp. 1289–1297, 2021.
- [21] J. Jiang, D. Pan, H. Ren, X. Jiang, C. Li, and J. Wang, "Self-supervised trajectory representation learning with temporal regularities and travel semantics," in *2023 IEEE 39th international conference on data engineering (ICDE)*. IEEE, 2023, pp. 843–855.
- [22] B. N. Patro and V. S. Agneeswaran, "Simba: Simplified mamba-based architecture for vision and multivariate time series," *arXiv preprint arXiv:2403.15360*, 2024.
- [23] A. Liang, X. Jiang, Y. Sun, and C. Lu, "Bi-mamba4ts: Bidirectional mamba for time series forecasting," *arXiv preprint arXiv:2404.15772*, 2024.
- [24] T. Zhou, Z. Ma, Q. Wen, X. Wang, L. Sun, and R. Jin, "Fedformer: Frequency enhanced decomposed transformer for long-term series forecasting," in *International conference on machine learning*. PMLR, 2022, pp. 27 268–27 286.
- [25] Y. Zhang and J. Yan, "Crossformer: Transformer utilizing cross-dimension dependency for multivariate time series forecasting," in *The eleventh international conference on learning representations*, 2022.
- [26] B. Lim and S. Zohren, "Time-series forecasting with deep learning: a survey," *Philosophical Transactions of the Royal Society A*, vol. 379, no. 2194, p. 20200209, 2021.
- [27] J. F. Torres, D. Hadjout, A. Sebaa, F. Martínez-Álvarez, and A. Troncoso, "Deep learning for time series forecasting: a survey," *Big Data*, vol. 9, no. 1, pp. 3–21, 2021.
- [28] G. Woo, C. Liu, A. Kumar, C. Xiong, S. Savarese, and D. Sahoo, "Unified training of universal time series forecasting transformers," *arXiv preprint arXiv:2402.02592*,

2024.

- [29] A. Gu and T. Dao, "Mamba: Linear-time sequence modeling with selective state spaces," *arXiv preprint arXiv:2312.00752*, 2023.
- [30] Q. Zhang, H. Wen, W. Yuan, C. Chen, M. Yang, S.-M. Yiu, and H. Yin, "Hmamba: Hyperbolic mamba for sequential recommendation," *arXiv preprint arXiv:2505.09205*, 2025.
- [31] Q. Zhang, L. Qu, H. Wen, D. Huang, S.-M. Yiu, N. Q. V. Hung, and H. Yin, "M2rec: Multi-scale mamba for efficient sequential recommendation," *arXiv preprint arXiv:2505.04445*, 2025.